Research Square

Preprints are preliminary reports that have not undergone peer review.
They should not be considered conclusive, used to inform clinical practice,
or referenced by the media as validated information.

Single-larva transcriptomics resolve phenotype-anchored *Na⁺ K⁺ ATPase* expression during first shell formation in Pacific oyster larvae under ocean acidification conditions

Marissa D. Wright-LaGreca
marissawrightlagreca@uvic.ca

Vancouver Island University

Karen D. Leask
Vancouver Island University

Laura M. Parker
Port Stephens Fisheries Institute

Timothy J. Green
Vancouver Island University

Research Article

Keywords: ocean acidification, bivalves, aquaculture, transcriptomics, biomineralization

Posted Date: August 28th, 2026

DOI: https://doi.org/10.21203/rs.3.rs-10607237/v1

License: This work is licensed under a Creative Commons Attribution 4.0 International License. Read Full License

Additional Declarations: No competing interests reported.

Abstract

Bivalve larvae are highly sensitive to ocean acidification (OA) conditions, a global climate shift that applies selective pressure on calcareous marine organisms. Although a growing body of work exists on the effects of OA on bivalve larvae, most studies rely on pooled-larval sampling, which may obscure gene expression patterns by including larvae with severely underdeveloped or deformed phenotypes, which are common in OA conditions but are unlikely to survive to metamorphosis. Here, we tested a combination of single-larva transcriptomic techniques to investigate the expression of a candidate gene previously shown to be upregulated in OA conditions, *Na^+ K^+ ATPase (NKA)*, in Pacific oyster larvae of known phenotypes. We found that upregulation of the *NKA* gene is detected primarily in larvae with a developed first shell (prodissoconch I), and was not pronounced in underdeveloped or deformed larvae, suggesting its expression reflects active shell formation under OA conditions, rather than a generalized stress response. Further, *NKA* mRNA was primarily localized along the dorsal shell hinge, the site of $CaCO_3$ deposition, substantiating its role in early shell development. This study provides a methodological framework for phenotype-anchored sampling to investigate the expressional signatures underpinning successful shell development in OA conditions.

1. Introduction

Excess anthropogenic carbon dioxide (CO_2) emissions are fundamentally altering ocean chemistry through a process known as ocean acidification (OA) (Barton et al., 2012; Allison and Bassett, 2015). In 2020 alone, an estimated 37.4 ± 2.9 gigatons of anthropogenic CO_2 was released into the atmosphere (Friedlingstein et al., 2022), with ~ 25% of this projected to be absorbed by the ocean over the coming centuries (Archer et al., 1997; Sabine et al., 2004; Friedlingstein et al., 2024), resulting in a predicted pH drop of up to 0.7 units by 2300 (Caldeira and Wickett, 2003). Increased CO_2 inputs alter seawater carbonate chemistry, specifically the saturation state of aragonite and calcite, the calcium carbonate ($CaCO_3$) polymorphs that calcareous organisms use to build their shells (Cao and Caldeira, 2008). This anthropogenic alteration of seawater chemistry makes it more difficult for calcareous organisms to build and maintain shells, thereby adding a selective pressure to calcareous organisms that may be ill-equipped to tolerate these rapidly changing marine environments.

The economic and ecological consequences of OA on calcareous organisms, including shellfish, are considerable. In terms of aquaculture, farming of marine bivalves accounted for 17.7 million tonnes of global aquaculture production in 2020, worth an estimated 29.8 billion USD globally [Food and Agriculture Organization of the United Nations (FAO), 2022]. Further, the ecosystem services provided by shelled organisms such as nutrient remediation and filter-feeding activities account for another estimated 6.47 billion USD per annum (van der Schatte Olivier et al., 2020). Beyond the economic impact, reduced viability of shellfish will have cascading effects on other marine organisms since many shellfish are keystone or habitat-forming species (Rodriguez-Perez et al., 2019). Under climate models projected for the next 80 years, the negative effects of OA on shellfish viability will likely be significant, with the survival of these important species dependent on adaptation and mitigation strategies (Stewart-Sinclair et al., 2020).

Bivalve larvae are particularly vulnerable to OA conditions, as they must rapidly build their initial shell from aragonite in the first days of life (Waldbusser et al., 2013). Aragonite undersaturation and low pH of OA seawater alters biomineralization pathways in the growing larvae, reducing larval shell growth and viability (Feely et al., 2009). Although inherently connected by the shell formation process, aragonite undersaturation and low pH create

distinct issues during shell formation: 1) substrate (CO_3^{2-}) availability and dissolution and 2) disruption of the internal pH conditions needed for crystal formation and other physiological processes, respectively (Dwyer and Burnett, 1996; Waldbusser et al., 2013). To date, substrate availability (i.e., $CaCO_3$ saturation or the availability of carbonate ions) and dissolution has generally been identified as the primary driver of negative impacts on shell formation in bivalve larvae following exposure to OA, with reduced pH being the secondary driver (Waldbusser et al., 2015). In the first 24–48 hours, bivalve larvae deposit a significant amount of aragonite (upwards of 90% of total body mass) to build their initial shell, called the prodissoconch I shell (Waldbusser et al., 2013). At this larval stage, shell growth is intrinsically linked to survival, and the inability to lay down a shell due to OA conditions will ultimately lead to mortality (Ventura et al., 2016). Aragonite saturation levels < 1.7 negatively impact shell development of bivalve larvae that use aragonite (Barton et al., 2015; Evans et al., 2019). OA susceptibility between larvae is varied both across (Campanati et al., 2018) and within species (Parker et al. 2012; Wright-LaGreca et al., 2022; Parker et al. 2025); suggesting adaptation, henceforth termed 'resiliency', to near-future seawater conditions is possible. This implies that, with increased knowledge behind the factors involved in resiliency to OA conditions, OA-resilient larvae can be selected for in aquaculture populations (quantitative genetics) or may be occurring naturally in wild populations (natural selection) (Tan and Zheng, 2020). A candidate gene underlying OA-resiliency encodes a *Na^+ K^+ ATPase (NKA*), which plays a central role in regulating internal pH by coupling with Na^+/H^+ exchangers and vacuolar-type H^+- ATPases to reduce intracellular H^+ concentrations (Melzner et al., 2009). Additionally, *NKA* creates an electrochemical gradient for powering transport of other molecules that may aid in shell deposition under aragonite-undersaturation. Previous studies have documented high *NKA* expression in OA seawater conditions (Ivanina et al., 2020; Wright-LaGreca et al., 2022); though reduced NKA enzyme activity in OA conditions has also been observed (Frieder et al., 2017), obscuring its role in OA-resiliency. Insights into the genes responsible for OA-resiliency is of great importance as they may be used as genetic biomarkers for selective breeding programs.

A major methodological limitation in larval 'omics (*e.g.*, genomics, transcriptomics, proteomics) is the use of "larval pooling": A technique involving the pooling of hundreds to thousands of larvae into a single sample. This is often necessary to achieve enough protein/nucleic acid content to measure changes in mRNA (Ramesh et al., 2019; Wright-LaGreca et al., 2022), protein abundance (Dineshram et al., 2016), enzyme activity (Frieder et al., 2017), or DNA genotyping (Durland et al., 2021). The main issue of pooled larval samples is that they can contain larvae at different developmental points: egg, trochophore, or early/late prodissoconch I stage, whereby gene expression and protein synthesis between these early stages has been shown to be drastically different (Liu et al., 2015). Additionally, phenotypic variability (*e.g.*, larvae with normal versus deformed shells) within a sample population may blur results. In OA conditions, the proportion of underdeveloped and deformed larvae are much greater (Wright-LaGreca et al., 2022). The expression of NKA and related transporters has been previously shown to peak during late trochophore stage in blue mussel (*Mytilus edulis*) larvae (Ramesh et al., 2019). Thus, the question arises if detected expressional signals in OA conditions are driven by a high proportion of underdeveloped or deformed larvae in pooled larval samples. This question informs if NKA expression is involved in proper development in OA conditions or instead is an expressional signature of samples containing large amounts of underdevelopment and/or larvae with severe shell deformities.

Phenotype-based selection of individual larvae combined with single-larva transcriptomic techniques, can elucidate gene expression trends under OA conditions without the use of larval pooling. Whole-mount FISH methods for mRNA localization have been utilized in *Mytilus galloprovincialis* embryos and larvae (Paganos et al., 2022) and single-animal RT-qPCR approaches have been successfully employed in zebrafish embryos (*Danio rerio*)

(de Jong et al., 2010) and *Caenorhabditis elegans* (Chauve et al., 2020). Phenotype-based selection followed by RNA sequencing has been utilized in *Mytilus californicus* to elucidate toxin biomarkers between normal and abnormal phenotypes following copper exposure (Hall and Gracey, 2021). As well, phenotype-based selection has been utilized to genotype individual *C. gigas* larvae based on size class to identify QTLs associated with fast growth (Pan et al., 2024). To our knowledge, neither technique has been applied to bivalve larvae to investigate genes believed to be involved in OA-resiliency.

Here, we aimed to test if the observed upregulation of a *sodium potassium (Na^+ K^+) ATPase* gene (denoted *NKA (1)*, GenBank #NM_011436470) in *C. gigas* larvae exposed to OA conditions ($\Omega_{Aragonite} < 1.7$) found in our previous study (Wright-LaGreca et al., 2022) is driven by a high concentration of severely underdeveloped or deformed larvae within pooled larval samples that are unlikely to survive past early developmental stages. Additionally, we aimed to approximate the site of *NKA (1)* mRNA localization, which can inform its role in OA conditions. Finally, we compare the expressional trends of select genes (n = 21 genes) encoding transport and shell matrix proteins involved in early shell formation between single and pooled larval sampling approaches. These results have direct implications for the use of *NKA (1)* as a genetic biomarker in OA selective breeding programs and can contribute more broadly to our fundamental understanding of shell formation, which remains a highly elusive “black box” due to its difficulty to measure and observe *in vivo* (Marin et al., 2007; Ramesh et al., 2018). This research provides a methodological framework for phenotype-anchored single-larva transcriptomics to elucidate the potential impact of sampling methods on our understanding and selection of individuals that are resilient to environmental stressors.

2. Materials and Methods

2.1 Seawater treatment and larval exposure

Seawater for each respective transcriptomic experiment (wmFISH and RT-qPCR), was collected from the BS17 collection site (Deep Bay, British Columbia; 49.474N, 124.758W), an area in the Northern Salish Sea that exhibits year-round OA conditions at low depths (Evans et al., 2019). During upwelling events, acidified seawater at these low depths contribute to corrosive conditions connected to adverse outcomes for shellfish health (Feely et al., 2008). We exploited this natural depth profile to create a control (5 m collection) and aragonite-undersaturated (70 m collection) seawater treatment, aimed to simulate upwelling events (Nordio et al., 2019; Wright-LaGreca et al., 2022). For carbonate chemistry analysis, triplicate seawater samples at both depths (5 and 70 m) were stored in sealed amber-glass bottles treated with saturated $HgCl_2$ to disrupt microbial activity. Temperature (°C) and salinity (ppt) were measured using a YSI Multilab 4010-2 W probe at the time of carbonate chemistry analyses following calibration with the YSI 2130 conductivity calibrator. Salinity and total alkalinity (TA) (μmol kg^{-1}) in this region have a linear relationship, where the equation developed by Evans et al., was used to calculate TA ($Alk_{inorganic}$ = Salinity*59.88 + 279.29) (2019). Seawater chemistry parameters were used to calculate aragonite saturation ($\Omega_{Aragonite}$) (CO2Sys, Pierrot et al., 2006). Seawater treatment names are based on relative aragonite saturation states (5m, high $\Omega_{Aragonite}$; 70m, low $\Omega_{Aragonite}$) as aragonite saturation state is the primer driver of the negative effects of OA on bivalve larvae (Waldbusser et al., 2013) and is standard convention (Nordio et al., 2019; Wright-LaGreca et al., 2022; Gurr et al., 2025). Carbonate chemistry metrics are reported in Table 1.

Table 1

Carbonate chemistry metrics of seawater treatments collected in Deep Bay, British Columbia (49.474N, 124.758W) known as the BS17 sampling station, at depths of 5 ("high $\Omega_{Aragonite}$") and 70 m ("low $\Omega_{Aragonite}$") below seawater surface. Seawater was collected across multiple dates for separate transcriptome experiments using either whole-mount fluorescent *in situ* hybridization (wmFISH) or reverse transcription quantitative real-time polymerase chain reaction (RT-qPCR) methods to investigate gene expression in aragonite-undersaturated ($\Omega_{Aragonite}$) relative to control conditions. Triplicate mean ± standard deviations are reported. NA = not applicable.

Treatment	Depth (m)	Temperature (°C)	pH_{NBS}	Salinity (ppt)	Total Alkalinity (µmol L)	Aragonite saturation ($\Omega_{Aragonite}$)	Method	Collection date
High $\Omega_{Aragonite}$	5	17.70 ± 0.08	8.45 ± 0.01	24.0 ± 0.05	1718 ± 3.46	2.56 ± 0.105	RT-qPCR	2021/06/21
Low $\Omega_{Aragonite}$	70	17.70 ± 0.05	7.81 ± 0.02	29.80 ± 0.00	2063 ± 0.00	1.36 ± 0.067	RT-qPCR	2021/06/21
High $\Omega_{Aragonite}$	5	18.07 ± 0.12	8.18 ± 0.02	27.67 ± 0.06	1935 ± 3.46	3.38 ± 0.066	wmFISH	2022/06/08
Low $\Omega_{Aragonite}$	70	17.73 ± 0.12	7.56 ± 0.06	29.13 ± 0.06	2023 ± 3.46	0.79 ± 0.103	wmFISH	2022/06/08

Larval breeding and seawater treatment exposure followed the protocol described in Wright-LaGreca et al., 2022. Larvae used for RT-qPCR and wmFISH analysis were generated from separate spawning events. Broodstock (parents) were sourced from the Vancouver Island University selective breeding program. Broodstock were sexed and gametes of selected parents were collected via strip spawning using a sterile disposable scalpel and gametes were washed with 5 µm-filtered seawater. Eggs were fertilized with ~ 3 mL of sperm solution in 1.5 L buckets and left for one hour to allow fertilization. Fertilization was confirmed by visualizing polar body formation with an Olympus compound microscope (10X). Fertilized egg solution was pipetted into 15 mL Eppendorf tubes that were subsequently filled to the top (limit air space) with either the control (5 m collected seawater, high $\Omega_{Aragonite}$) or the aragonite undersaturated treatment (70 m collected seawater, low $\Omega_{Aragonite}$) to achieve a concentration of ~ 300 eggs/tube (5 replicates per seawater treatment), and incubated at 24°C for 24 hrs. At the end of this time, tubes were spun down at 15,000 RPM for 6 minutes and seawater was removed. Larval samples used for wmFISH analysis were stored in 1 mL of 10% neutral-buffered formalin until RNA probe hybridization. Selection of individual larva for single-larva transcriptomics and pooled sampling methods are described in section 2.3. All invertebrate handling (Category of Invasiveness - A) was approved by Vancouver Island University's Animal Care Committee (file #101943–12589).

2.2 Probe formation and specimen hybridization for whole-mount fluorescent in situ hybridization

The FISH Tag RNA Multicolor Kit with Alexa Fluor™ dyes (Invitrogen; F32956) was used to synthesize Fluorescent Dye-Labeled RNA probes, where the protocol was largely followed (https://documents.thermofisher.com/TFS-Assets/LSG/manuals/mp32956.pdf). Optimization of this protocol for whole-larval tissue-type are described, largely concerning hybridization steps, where the Thermo Fisher protocol was designed for *Drosophila melanogaster* embryos. After 24 hrs post-fertilization, *C. gigas* larvae are significantly smaller than *D. melanogaster* embryos (70–100 µm compared to 500 µm length, respectively); however, the presence of the prodissoconch I shell was suspected to require hybridization optimization to ensure probe penetration. RNA probes were designed

for the housekeeping gene, *elongation factor unit alpha* (*EFU*) (Genbank #AB122066), and *Na^+ K^+ATPase* [*NKA (1)*] (Genbank ID: XM_011436470) with the Alexa Fluor® (fluorophore) 594 and 647, respectively. Probe penetration was measured by the attachments of the *EFU* probe (expressed in all cells) throughout larval tissue. Following probe synthesis, RNA probe concentrations were measured with the Eppendorf Biospectrometer® (A_{260} and A_{dye} wavelength) and diluted with molecular-grade water to a concentration of 1 µg/µL. As recommended for pre-hybridization optimization (step 11.12), proteinase K stock concentrations from 5 to 50 µg/mL were tested, where 15 µg/mL was selected for optimal probe penetration while maintaining tissue integrity. Additionally, incubation times ranging from 15–32 hrs were tested, where 15 hrs incubation at 55 °C achieved optimal probe hybridization. Incubation steps were conducted in 0.8 mL tubes in an Eppendorf® Mastercycler® Nexus Thermo Cycler.

Following post-hybridization washing steps, probe-labelled larvae were imaged with the Leica Thunder 3D Imager at 64X magnification. Due to the effects of hybridization steps on tissue quality, deformed versus normal D-larval phenotypes were difficult to interpret and thus phenotypic data were not analysed. The Z-Stack imaging feature was used to create 3D images of larvae (n = 40 Z-stacks across 8.52 µm depth). All images were taken with the same exposure and gain settings (500 milliseconds and 1, respectively) with instant and small-volume computational clearing to reduce non-specific fluorescence. Fluorescence quantification was recorded for both fluorophores (594 and 647 nm) by selecting the focal transverse larval section following Z-stack imaging and using the region of interest (ROI) (71 x 81 µm) feature to select the area of the larvae and recording fluorescence at the nearest wavelength on our instrument (560 and 642 nm, respectively) for each larval image (n = 15 in aragonite-undersaturated treatment, n = 14 in control treatment). To normalize fluorescence levels, relative fluorescence of *NKA (1)* (Alexa 647) was standardized against *EFU* (Alexa 594) housekeeping gene fluorescence levels using an *NKA (1)*/*EFU* ratio calculation. The *NKA (1)*/*EFU* ratio values were used for subsequent statistical analysis. A control larval sample was subjected to all hybridization protocols except for the addition of the fluorescence probes and compared to other samples to test for the effects of autofluorescence on mRNA localization. Fluorescence data was exported as a CSV file.

2.3 Single and pooled larval RT-qPCR

In addition to the *NKA (1)* gene, 20 other previously investigated genes were selected for comparing RT-qPCR of single and pooled larval samples (Wright-LaGreca et al., 2022). For single larval sampling, following seawater exposure for 24 hrs, live individual larvae from either seawater treatment were selected with a 10 µL pipette based on phenotype (trochophore, deformed D-larva, or normal D-larva) using an Olympus SZX16 Stereo Microscope with a 10X eyepiece (WHN10X-H/22) and a 0.5X objective for visualization with the magnification ranging from 3.5 to 57.5X depending on the manually adjusted zoom setting during sampling. Individual larvae were placed in individual wells of a 96-well plate with sample location recorded. Phenotypes were visually classified as being a trochophore (ciliated and unformed shell), or having a normal prodissoconch I (PI) shell or deformed PI shell, where shell deformities include a protruding mantle, indented margin, convex hinge, or cupped shell-shape as described in our previous publication (Wright-LaGreca et al., 2022, adapted from Ventura et al., 2016). To avoid collecting samples (individual larvae) at substantially different time points, sample collection was limited to approximately two hrs, allowing for the collection of six larvae in the control treatment (phenotypes: n = 5 normal PI; n = 1 trochophore) and 12 larvae in the low $\Omega_{Aragonite}$ (phenotypes: n = 6 normal PI; n = 3 deformed PI; n = 3 trochophores). As noted, sample size was constrained by sample collection time, and as well, no deformed PI and only one underdeveloped (trochophore) larva were observed in high $\Omega_{Aragonite}$, which reflects proper development in normal seawater conditions (not OA) but limits phenotypic comparisons across seawater treatments. Triplicate pooled-larval samples from the control and aragonite-undersaturated treatments were collected in 15 mL

Eppendorf tubes, pelleted by centrifugation, and excess seawater was poured out. Larval samples were preserved at – 80 °C until RNA preparation.

For single larval samples, RNA amplification and reverse transcription was performed using the QIAGEN Whole Transcriptome Analysis (WTA) REPLI-g® Single Cell kit (#150063). Pooled-larval samples were extracted using a TRIzol LS reagent (Thermo Fisher) and reverse transcription was performed using the BIO-RAD iScript cDNA synthesis kit with random primers. Real Time Quantitative PCR (RT-qPCR) with BIO-RAD SsoAdvanced Universal SYBR Green Supermix (5 µL), selected forward and reverse primers (1 µL each), and cDNA (3 µL) was performed with the following protocol: 95 °C for 2 mins, and 40 cycles of 95 °C for 10 s (denaturation), 60 °C for 30 s (elongation). The $2^{-\Delta\Delta Ct}$ method was used to infer relative expression to the housekeeping gene, Elongation Factor Unit 1-alpha (*EFU*) (GenBank #AB122066).

2.4 Statistical analysis

All statistical analysis was conducted in R Studio software (v4.3.3). wmFISH experimental results (*NKA (1)*/*EFU* ratio values) and larval size (length in µm) were analyzed using a Student's *t*-test, where data met normality (Shapiro-Wilk normality test) and homogeneity of variance (Levene's test) assumptions ($p > 0.05$ across all tests) (stats R package; R Core Team, 2026). A Pearson's correlation test was used to test for the correlation between *NKA (1)* expression and size in both seawater conditions. A Cook's distance diagnostic plot (residuals vs leverage) was used to identify outliers for correlation tests.

Normalized Cq data from single and pooled larval samples for RT-qPCR analysis were transformed [Log(X + 1)] and Brays-Curtis resemblance matrix was generated to perform a PERMANOVA analysis with the factors: Seawater treatment (high or low $\Omega_{Aragonite}$) and phenotype (trochophore, deformed PI, or normal PI). To investigate *NKA (1)* expression (Cq) between treatment and/or phenotype groups using single and pooled larval methods, an Exact Two-Sample Fisher-Pitman Permutation test was utilized due to low sample size and non-normal data (coin R package; Hothorn et al., 2006). To compare findings of single or pooled larval sampling methods, log-fold change in expression of each gene in low $\Omega_{Aragonite}$ relative to high $\Omega_{Aragonite}$ conditions was calculated and the cor.test function (stats R package) with a Spearman's *p* correlation coefficient was used to test for association between paired samples (each gene) between methods. Plots were generated with ggplot2 (Wickham, 2016) with color scales ("magma") from the viridis R package (Garnier et al., 2018).

3. Results

3.1 Quantification of NKA (1) mRNA levels and localization using whole-mount fluorescent in situ hybridization

The wmFISH results indicate significant differences in relative *NKA (1)* expression between larvae reared in high and low $\Omega_{Aragonite}$ [$t(40) = 2.85$, $p = 0.007$], corresponding to a 21.4% increased relative *NKA (1)* expression in aragonite-undersaturated (low $\Omega_{Aragonite}$) conditions. Larvae from the low $\Omega_{Aragonite}$ treatment were significantly smaller than larvae from high $\Omega_{Aragonite}$ (72.94 ± 4.52 and 76.69 ± 5.72, respectively) ($t(4) = -2.33$, $p = 0.025$) (Fig. 1). Using all data points, we found a positive Pearson's correlation between *NKA (1)* expression and size in low $\Omega_{Aragonite}$ conditions [$r = 0.483$, $t(19) = 2.40$, $p = 0.027$ (CI: 0.064, 0.757)] but no correlation in high $\Omega_{Aragonite}$ conditions [$r = -0.18$, $t(19) = -0.796$, $p = 0.446$ (CI: -0.567, 0.273)]; however, when inspecting for outliers, this

significant correlation was driven by a single outlier, whereby when it was removed, no significant correlation was present [r = 0.257, *t*(18) = 1.13, *p* = 0.275 (CI: -0.210, 0.628)].

Images of wmFISH (Figs. 2 and 3) indicate sites of *NKA (1)* expression relative to *EFU* expression (expressed in all cells). *NKA (1)* is largely expressed on the shell margins, particularly on the dorsal shell edge (Fig. 2 and Supplemental Video 1). No visual differences in *NKA (1)* mRNA localization were apparent between samples in high and low $\Omega_{Aragonite}$ conditions.

3.2 RT-qPCR-based single and pooled larval transcriptomics

PERMANOVA analysis indicated global gene expression of the 21 selected genes was not significantly different across seawater treatment [F(1) = 1.66, *p* = 0.084] or larval phenotype [F(2) = 0.680, *p* = 0.863] using single-larva RT-qPCR based methods. Similarly, global gene expression was not significantly different between seawater treatment in pooled larval samples (F(1) = 2.57, *p* = 0.100). Examination of individual genes indicated two genes were marginally significantly different between seawater treatments: *SLC4 (3)* was downregulated in low $\Omega_{Aragonite}$ conditions (Z = 1.79, *p* = 0.05) and *NKA (1)* was upregulated in high $\Omega_{Aragonite}$ (Z = -1.65, *p* = 0.05) in pooled larval samples. When analyzing gene expression using single-larva RT-qPCR based methods, no significant differences in gene expression of any of the 21 genes were detected between larval phenotype or seawater treatment. Pooled and single larval sampling methods for RT-qPCR indicate similar trends in the upregulation of *NKA (1)* in low $\Omega_{Aragonite}$ conditions (Fig. 3).

Across all genes, the test for association between RT-qPCR based methods indicated no significant global concordance between single and pooled larval sampling methods (S = 1410, rho = 0.084, *p* = 0.716). When examining individual genes, several supported concordant direction responses across methods, notably, both methods indicate only one gene upregulated in low $\Omega_{Aragonite}$ conditions, *NKA (1)*, and 10 genes downregulated in OA [*peptidase, nacrein 1, pif-177, nacrein 2, calmodulin 2, SLC4 (4), papilin, NKA (2), nacrein (3), chitin-synthase*]. Conversely, the relative expression between seawater treatments of 10 genes was not consistent between sampling methods, all of which were upregulated in OA conditions using the single larval approach but downregulated in pooled larval samples (Fig. 4). Some notable differences in the strength of expression directionality include *perlucin 2*, *tyrosinase*, and *nacrein 5*. However, as previously mentioned, none of these genes were significantly upregulated in low $\Omega_{Aragonite}$ conditions following permutation testing.

4. Discussion

Ocean acidification (OA) is a major anthropogenic threat to calcareous marine organisms, particularly those that build their shell from the aragonite polymorph of $CaCO_3$, such as Pacific oyster larvae, which becomes severely undersaturated under OA conditions (Barton et al., 2015). Pooled larval samples are commonly used to measure gene expression as it is often needed to achieve sufficient RNA yields; however, a major methodological issue is that pooled samples contain many larvae at various developmental stages and of different phenotypes, which is especially evident in aragonite-undersaturated conditions. Previous research suggested a high expression of a gene [*NKA (1)*] encoding a Na^+ K^+ATPase transporter, in aragonite-undersaturated conditions (De Wit et al., 2018; Wright-LaGreca et al., 2022); however, it is unclear if this expression is driven by underdeveloped (eggs or trochophores) or developed larvae but with abnormal (termed “deformed”) phenotypes, that are present in high numbers in aragonite-undersaturated conditions, but are not expected to survive to metamorphosis. Thus, it is

unclear if high *NKA (1)* expression in aragonite-undersaturated conditions reflects adaptation, being expressed in larvae that successfully develop in OA conditions, or instead, is upregulated in underdeveloped or deformed larvae. Using a combination of whole-mount fluorescent *in situ* hybridization (wmFISH) and RT-qPCR based methods to investigate differences in gene expression between sampling methods (single or pooled), we substantiate that *NKA (1)* expression is upregulated in aragonite-undersaturated conditions (low $\Omega_{Aragonite}$ treatment) in larvae with a developed prodissoconch I shell. Further, mRNA localization using wmFISH indicate *NKA (1)* is primarily expressed on the dorsal edge of the shell at 24 hours post-fertilization, the site of prodissoconch I shell formation (Min et al., 2023), supporting its involvement in initial shell formation, reflecting the importance of ion-transport during early physiological processes.

Using wmFISH methods, we detected a ~ 21% upregulation of the *NKA (1)* gene in larvae with a developed prodissoconch I shell that were reared in aragonite-undersaturated conditions. Additionally, we found that larvae used for wmFISH analyses were ~ 5% smaller in aragonite-undersaturated conditions. Using wmFISH methods, we were able to distinguish between underdeveloped (trochophore) and developed (prodissoconch I shell) larvae; however, it was deemed unreliable to compare normal and deformed shell-types for wmFISH analysis due to the potential impact of probe-hybridization and wash steps on shell integrity. Single-larva RT-qPCR based methods were tested as an alternative to compare larval phenotypes (normal, deformed, or underdeveloped). Although we had a limited sample size to investigate *NKA (1)* expression in aragonite-undersaturated conditions between larval phenotypes using RT-qPCR based methods because selecting individual larvae was time intensive and thus sample size was constrained to avoid comparing individuals at different developmental points, relative *NKA (1)* expression in underdeveloped larvae (trochophore) was low across all collected samples (n = 4, $1.01 \pm 0.20 \times 10^{-3}$). Additionally, *NKA (1)* expression in larvae with deformed prodissoconch I shells was variable in aragonite-undersaturated conditions (n = 3, $6.36 \pm 9.72 \times 10^{-3}$) but not pronounced compared to larvae with normal prodissoconch I shells (n = 6, $8.10 \pm 13.3 \times 10^{-3}$).

We found that phenotype-based selection for single-larva RT-qPCR based methods did not further elucidate expressional patterns in the 21 tested genes, including *NKA (1)*, compared to pooled sampling methods. Although 10 genes were found to have different expressional trends (up or downregulation in low $\Omega_{Aragonite}$) between sampling methods, none of these genes were differentially expressed using either sampling method. Single-larva RT-qPCR based methods indicate high variability of individual larvae in the expression of selected genes, with no clear trends in expression between normal and deformed phenotypes. This variability may be influenced by limited sample size (n = 6 larvae in control; n = 12 larvae in aragonite-undersaturated conditions). Conversely, expressional variability between individuals may reflect a true biological effect, which may contribute to observed variability between pooled larvae replicates and inconclusive expressional trends. We again found that the upregulation of *NKA (1)* was the most notable findings across both sampling methods, supporting results from wmFISH analyses and previous studies (De Wit et al., 2018; Wright-LaGreca et al., 2022).

High levels of shell deposition occur on the shell hinge and mantle edge at 24 hrs post-fertilization (Min et al., 2023). Bivalve larvae can modify internal pH and CO_3^{2-} ($CaCO_3$ precursor) within the calcifying space to promote calcification (Ramesh et al., 2017). Our results indicate *NKA* mRNA localization largely along the dorsal shell edge (shell hinge). At the trochophore stage following evagination, outer epithelial cells secrete organic matter known as the periostracum around the periphery (Ramesh et al., 2018). The periostracum provides an outer, protective barrier that enables internal cellular modifications and subsequent shell deposition (Hűning et al., 2013). Following this, the deposition of $CaCO_3$ occurs in the extrapallial space, located between the periostracum and mantle edge

(Mouëza et al., 2006). These results provide support that NKA activity is involved in $CaCO_3$ deposition during initial shell development. We found no evidence of variations in *NKA* mRNA localization between seawater treatments, and instead, upregulation of *NKA* was the primary signature of aragonite-undersaturation.

NKA activity has been linked to fast growth, explaining ~ 43% of variations in growth between pedigreed *C. gigas* families (Pan et al., 2016). Fast growth at the larval stage has been shown to be involved in genetically determined resiliency to aragonite-undersaturated conditions (Parker et al. 2012; Nordio et al., 2021). This comes at an energetic cost, whereby *in vitro* enzymatic analysis indicates ion-regulatory activities account for 12 to 34% of total ATP allocation (Pan et al., 2016). High NKA activity may promote fast growth in aragonite-undersaturated conditions by creating the electrochemical gradient needed for increased amino acid transport (Leong and Manahan, 1997; Wright and Manahan, 1989). Amino acids are a non-endogenous energy resource that can be taken up by non-feeding larvae in a process called epidermal amino acid transport (Stephens, 1988). Amino acids are absorbed from seawater in non-feeding larvae at an even a higher rate than feeding stages (e.g., 3–5 times higher for glycine) (Reish and Stephens, 1969) and catabolized for energy (Dineshram et al., 2015). The catabolism of amino acids results in significant increases in internally derived CO_2 (Manahan, 1983), which fuels the activity of carbonic anhydrases to produce bicarbonate (HCO_3), a precursor to calcium carbonate ($CaCO_3$). Amino acid transport capacity has been observed to have a genetic basis and to be correlated with growth potential in *C. gigas* (Pan et al., 2015). Thus, high amino acid transport, potentially fuelled by ion-transporters such as NKA, may support growth in aragonite-undersaturated conditions by increasing internally derived $CaCO_3$ concentrations. We recommend future studies quantify gene expression or enzyme activity of amino acid transports in tandem with ion transporters such as *NKA* using phenotype-anchored, single larval 'omic methods.

5. Conclusion

In the height of a rapidly changing marine environment, ocean acidification threatens marine organisms, particularly those that build a $CaCO_3$ shell. In earth's history, rapid increases in CO_2 levels have occurred with massive extinctions, and thus, current global changes will also pose significant dangers to modern marine life (Pandolfi et al., 2011; Kelly and Hofmann, 2013). Knowledge of the genes involved in survival in ocean acidified conditions can play a critical role in mitigation and conservation strategies. Few studies have investigated expressional signatures of individual larvae with known phenotypes. Here we tested two methods for quantifying and localizing gene expression of individual larvae. With these methods, we substantiate high expression of a *Na^+ K^+ ATPase (NKA*) previously found to be upregulated in aragonite-undersaturated conditions in individual larvae, concluding that *NKA* upregulation is observed in larvae that develop a shell, and not by severely underdeveloped larvae. This work provides a methodological framework for future work investigating genes involved in resiliency against ocean acidification conditions at the single larval level.

Declarations

7. Conflicts of Interest

Authors report no competing interests.

Author Contribution

T.G. developed the experimental framework. M.W.L. and K.L. performed the experiments and collected data. M.W.L. performed statistical analysis and created figures. M.W.L., T.G., and L.P. wrote the main manuscript text. All authors reviewed the manuscript and provided manuscript edits.

6. Acknowledgements

M.D. Wright-LaGreca and T.J. Green are supported by funding provided to T.J. Green from the Canada Research Chair Program (CRC, #950-231856) and Natural Sciences and Engineering Research Council (NSERC, #2018–06761). L.M. Parker is supported by the ARC Discovery Indigenous grants (IN190100051 and IN220100054).

Data Availability

Data and code is available at the GitHub repository: https://github.com/MarissaLag/Data-analysis-for-single-larval-transcriptomics.

References

1. Allison, E. H. and Bassett, H. R., 2015. Climate change in the oceans: Human impacts and responses, *Science, 350*(6262), pp. 778-782.
2. Archer, D., Kheshgi, H. and Maier-Reimer, E., 1997. Multiple timescales for neutralization of fossil fuel CO2. *Geophysical Research Letters*, *24*(4), pp.405-408.
3. Barton, A., Hales, B., Waldbusser, G. G., Langdon, C. and Feely, R. A., 2012. The Pacific oyster, *Crassostrea gigas*, shows negative correlation to naturally elevated carbon dioxide levels: Implications for near-term ocean acidification effects. *Limnology and Oceanography, 57*(3), pp. 698-710.
4. Barton, A., Waldbusser, G.G., Feely, R.A., Weisberg, S.B., Newton, J.A., Hales, B., Cudd, S., Eudeline, B., Langdon, C.J., Jefferds, I. and King, T., 2015. Impacts of coastal acidification on the Pacific Northwest shellfish industry and adaptation strategies implemented in response. *Oceanography*, *28*(2), pp.146-159.
5. Caldeira, K. and Wickett, M.E., 2003. Anthropogenic carbon and ocean pH. *Nature*, *425*(6956), pp.365-365.
6. Campanati, C., Dupont, S., Williams, G.A. and Thiyagarajan, V., 2018. Differential sensitivity of larvae to ocean acidification in two interacting mollusc species. *Marine environmental research*, *141*, pp.66-74.
7. Cao, L. and Caldeira, K., 2008. Atmospheric CO2 stabilization and ocean acidification. *Geophysical Research Letters*, *35*(19).
8. Chauve, L., Le Pen, J., Hodge, F., Todtenhaupt, P., Biggins, L., Miska, E.A., Andrews, S. and Casanueva, O., 2020. High-throughput quantitative RT-PCR in single and bulk *C. elegans* samples using nanofluidic technology. *Journal of visualized experiments: JoVE, 159*, pp.10-3791.
9. de Jong, M., Rauwerda, H., Bruning, O., Verkooijen, J., Spaink, H.P. and Breit, T.M., 2010. RNA isolation method for single embryo transcriptome analysis in zebrafish. *BMC research notes*, *3*(1), pp.73.
10. De Wit, P., Durland, E., Ventura, A. and Langdon, C.J., 2018. Gene expression correlated with delay in shell formation in larval Pacific oysters (*Crassostrea gigas*) exposed to experimental ocean acidification provides insights into shell formation mechanisms. *BMC genomics*, *19*(1), pp.160.
11. Dineshram, R., Sharma, R., Chandramouli, K., Yalamanchili, H.K., Chu, I. and Thiyagarajan, V., 2015. Comparative and quantitative proteomics reveal the adaptive strategies of oyster larvae to ocean

acidification. Proteomics, 15, pp. 4120-4134.

12. Dineshram, R., Chandramouli, K., Ko, G.W.K., Zhang, H., Qian, P.Y., Ravasi, T. and Thiyagarajan, V., 2016. Quantitative analysis of oyster larval proteome provides new insights into the effects of multiple climate change stressors. *Global Change Biology*, *22*(6), pp.2054-2068.
13. Durland, E., De Wit, P., Meyer, E. and Langdon, C., 2021. Larval development in the Pacific oyster and the impacts of ocean acidification: Differential genetic effects in wild and domesticated stocks. *Evolutionary Applications*, *14*(9), pp.2258-2272.
14. Dwyer, III, J.J. and Burnett, L.E., 1996. Acid-base status of the oyster *Crassostrea virginica* in response to air exposure and to infections by *Perkinsus marinus*. *The Biological Bulletin*, *190*(1), pp.139-147.
15. Evans, W., Pocock, K., Hare, A., Weekes, C., Hales, B., Jackson, J., Gurney-Smith, H., Mathis, J.T., Alin, S.R. and Feely, R.A., 2019. Marine CO2 patterns in the northern Salish Sea. *Frontiers in Marine Science*, *5*, pp.536.
16. Food and Agriculture Organization of the United Nations (FAO), 2022. The State of World Fisheries and Aquaculture 2022: Towards Blue Transformation. Rome: FAO.
17. Feely, R.A., Sabine, C.L., Hernandez-Ayon, J.M., Ianson, D. and Hales, B., 2008. Evidence for upwelling of corrosive" acidified" water onto the continental shelf. *Science*, *320*(5882), pp.1490-1492.
18. Feely, R.A., Doney, S.C. and Cooley, S.R., 2009. Ocean acidification: Present conditions and future changes in a high-CO_2 world. *Oceanography*, *22*(4), pp.36-47.
19. Frieder, C.A., Applebaum, S.L., Pan, T.C.F., Hedgecock, D. and Manahan, D.T., 2017. Metabolic cost of calcification in bivalve larvae under experimental ocean acidification. *ICES Journal of Marine Science*, *74*(4), pp.941-954.
20. Friedlingstein, P., Jones, M.W., O'sullivan, M., Andrew, R.M., Bakker, D.C., Hauck, J., Le Quéré, C., Peters, G.P., Peters, W., Pongratz, J. and Sitch, S., 2022. Global carbon budget 2021. *Earth System Science Data*, *14*(4), pp.1917-2005.
21. Friedlingstein, P., O'sullivan, M., Jones, M.W., Andrew, R.M., Hauck, J., Landschützer, P., Le Quéré, C., Li, H., Luijkx, I.T., Olsen, A. and Peters, G.P., 2024. Global carbon budget 2024. *Earth System Science Data Discussions*, *2024*, pp.1-133.
22. Garnier, S., Ross, N., Rudis, B., Sciaini, M., Camargo, A.P. and Scherer, C., 2018. Package 'viridis'. *Colorblind-friendly color maps for R*.
23. Gurr, S.J., Meseck, S.L., Bernatchez, G., Redman, D., Dixon, M.S., Guy, L., MacDonald, A., Stiles, S. and McFarland, K., 2025. Transcriptome-To-Phenome Response of Larval Eastern Oysters Under Multiple Drivers of Aragonite Undersaturation. *Ecology and Evolution*, *15*(2), p.e70953.
24. Hall, M.R. and Gracey, A.Y., 2021. Single-larva RNA sequencing identifies markers of copper toxicity and exposure in early *Mytilus californianus* larvae. *Frontiers in Physiology, 12*, pp.647482.
25. Hothorn, T., Hornik, K., Van De Wiel, M.A. and Zeileis, A., 2006. A lego system for conditional inference. *The American Statistician*, *60*(3), pp.257-263.
26. Hüning, A.K., Melzner, F., Thomsen, J., Gutowska, M.A., Krämer, L., Frickenhaus, S., Rosenstiel, P., Pörtner, H.O., Philipp, E.E. and Lucassen, M., 2013. Impacts of seawater acidification on mantle gene expression patterns of the Baltic Sea blue mussel: implications for shell formation and energy metabolism. *Marine Biology*, *160*(8), pp.1845-1861.
27. Ivanina, A.V., Jarrett, A., Bell, T., Rimkevicius, T., Beniash, E. and Sokolova, I.M., 2020. Effects of seawater salinity and pH on cellular metabolism and enzyme activities in biomineralizing tissues of marine bivalves.

Comparative Biochemistry and Physiology Part A: Molecular and Integrative Physiology, *248*, pp.110748.

28. Kelly, M.W. and Hofmann, G.E., 2013. Adaptation and the physiology of ocean acidification. *Functional Ecology*, *27*(4), pp.980-990.
29. Leong, P.K.K. and Manahan, D.T., 1997. Metabolic importance of Na+/K+-ATPase activity during sea urchin development. *Journal of experimental biology*, *200*(22), pp.2881-2892.
30. Liu, J., Yang, D., Liu, S., Li, S., Xu, G., Zheng, G., Xie, L. and Zhang, R., 2015. Microarray: a global analysis of biomineralization-related gene expression profiles during larval development in the pearl oyster, *Pinctada fucata*. *BMC genomics*, *16*(1), pp.325.
31. Manahan, D.T., 1983. The uptake and metabolism of dissolved amino acids by bivalve larvae. *The Biological Bulletin, 164*, pp. 236-250.
32. Marin, F., Luquet, G., Marie, B. and Medakovic, D., 2007. Molluscan shell proteins: primary structure, origin, and evolution. *Current topics in developmental biology*, *80*, pp.209-276.
33. Melzner, F., Gutowska, M.A., Langenbuch, M., Dupont, S., Lucassen, M., Thorndyke, M.C., Bleich, M. and Pörtner, H.O., 2009. Physiological basis for high CO 2 tolerance in marine ectothermic animals: pre-adaptation through lifestyle and ontogeny?. *Biogeosciences*, *6*(10), pp.2313-2331.
34. Min, Y., Li, Q. and Yu, H., 2023. Characterization of larval shell formation and *CgPOU2F1, CgSox5*, and *CgPax6* gene expression during shell morphogenesis in *Crassostrea gigas*. *Comparative Biochemistry and Physiology Part B: Biochemistry and Molecular Biology*, *263*, pp.110783.
35. Mouëza, M., Gros, O. and Frenkiel, L., 2006. Embryonic development and shell differentiation in *Chione cancellata* (Bivalvia, Veneridae): an ultrastructural analysis. *Invertebrate Biology*, *125*(1), pp.21-33.
36. Nordio, D., Khtikian, N., Andrews, S., Bertotto, D., Leask, K. and Green, T., 2021. Adaption potential of Crassostrea gigas to ocean acidification and disease caused by *Vibrio harveyi*. *ICES Journal of Marine Science*, *78*(1), pp.360-367.
37. Paganos, P., Caccavale, F., La Vecchia, C., D'Aniello, E., D'Aniello, S. and Arnone, M.I., 2022. FISH for all: A fast and efficient fluorescent *in situ* hybridization (FISH) protocol for marine embryos and larvae. *Frontiers in Physiology*, *13*, pp.878062.
38. Pan, T.C.F., Applebaum, S.L. and Manahan, D.T., 2015. Experimental ocean acidification alters the allocation of metabolic energy. *Proceedings of the National Academy of Sciences, 112*, pp. 4696-4701.
39. Pan, T.C.F., Applebaum, S.L., Lentz, B.A. and Manahan, D.T., 2016. Predicting phenotypic variation in growth and metabolism of marine invertebrate larvae. *Journal of Experimental Marine Biology and Ecology*, *483*, pp.64-73.
40. Pan, Y., Jiang, F., Shaw, R.K., Sun, J., Li, L., Yin, X., Bi, Y., Kong, J., Zong, H., Gong, X. and Ijaz, B., 2024. QTL mapping and genome-wide association analysis reveal genetic loci and candidate gene for resistance to gray leaf spot in tropical and subtropical maize germplasm. *Theoretical and Applied Genetics*, *137*(12), pp.266.
41. Pandolfi, J.M., Connolly, S.R., Marshall, D.J. and Cohen, A.L., 2011. Projecting coral reef futures under global warming and ocean acidification. *Science*, *333*(6041), pp.418-422.
42. Parker, L.M., Ross, P.M., O'Connor, W.A., Borysko, L., Raftos, D.A. and Pörtner, H.O., 2012. Adult exposure influences offspring response to ocean acidification in oysters. *Global change biology*, *18*(1), pp. 82-92.
43. Parker, L.M., Scanes, E., O'Connor, W.A., Dove, M., Vengatesen, T., Roberts, S. and Ross, P.M., 2025. Transgenerational plasticity responses differ across genetically distinct families in the Sydney rock oyster, *Saccostrea glomerata*. *Marine Environmental Research*, pp.107540.

44. Pierrot, D., Lewis, E., and Wallace, D. W. R., 2006. MS Excel program developed for CO_2 system calculations, ORNL/CDIAC-105a, Carbon Dioxide Information Analysis Center, Oak Ridge National Laboratory, U.S. Department of Energy, Oak Ridge, Tennessee, https://doi.org/10.3334/CDIAC/otg.CO2SYS_XLS_CDIAC105a.
45. R Core Team, 2026. R: A Language and Environment for Statistical Computing. R Foundation for Statistical Computing, Vienna, Austria. <https://www.R-project.org/>.
46. Ramesh, K., Hu, M.Y., Thomsen, J., Bleich, M. and Melzner, F., 2017. Mussel larvae modify calcifying fluid carbonate chemistry to promote calcification. *Nature Communications*, *8*(1), pp.1709.
47. Ramesh, K., Melzner, F., Griffith, A.W., Gobler, C.J., Rouger, C., Tasdemir, D. and Nehrke, G., 2018. *In vivo* characterization of bivalve larval shells: a confocal Raman microscopy study. *Journal of the Royal Society Interface*, *15*(141).
48. Ramesh, K., Yarra, T., Clark, M.S., John, U. and Melzner, F., 2019. Expression of calcification-related ion transporters during blue mussel larval development. *Ecology and Evolution*, *9*(12), pp.7157-7172.
49. Reish, D.J. and Stephens, G.C., 1969. Uptake of organic material by aquatic invertebrates: The influence of age on the uptake of glycine-C14 by the polychaete *Neanthes arenaceodentata*. *Marine Biology*, *3*(4), pp.352-355.
50. Rodriguez-Perez, A., James, M., Donnan, D.W., Henry, T.B., Møller, L.F. and Sanderson, W.G., 2019. Conservation and restoration of a keystone species: Understanding the settlement preferences of the European oyster (*Ostrea edulis*). *Marine pollution bulletin*, *138*, pp. 312-321.
51. Sabine, C.L., Feely, R.A., Gruber, N., Key, R.M., Lee, K., Bullister, J.L., Wanninkhof, R., Wong, C.S.L., Wallace, D.W., Tilbrook, B. and Millero, F.J., 2004. The oceanic sink for anthropogenic CO2. *Science, 305*, pp. 367-371.
52. Stephens, G.C., 1988. Epidermal amino acid transport in marine invertebrates. *Biochimica et Biophysica Acta (BBA)-Reviews on Biomembranes*, *947*(1), pp.113-138.
53. Stewart-Sinclair, P.J., Last, K.S., Payne, B.L. and Wilding, T.A., 2020. A global assessment of the vulnerability of shellfish aquaculture to climate change and ocean acidification. *Ecology and evolution, 10,* pp. 3518-3534.
54. Tan, K. and Zheng, H., 2020. Ocean acidification and adaptive bivalve farming. *Science of the Total Environment*, *701*, pp.134794.
55. Ventura, A., Schulz, S. and Dupont, S., 2016. Maintained larval growth in mussel larvae exposed to acidified under-saturated seawater. *Scientific Reports*, *6*(1), pp.1-9.
56. Waldbusser, G.G., Brunner, E.L., Haley, B.A., Hales, B., Langdon, C.J. and Prahl, F.G., 2013. A developmental and energetic basis linking larval oyster shell formation to acidification sensitivity. *Geophysical Research Letters*, *40*(10), pp.2171-2176.
57. Waldbusser, G.G., Hales, B., Langdon, C.J., Haley, B.A., Schrader, P., Brunner, E.L., Gray, M.W., Miller, C.A., Gimenez, I. and Hutchinson, G., 2015. Ocean acidification has multiple modes of action on bivalve larvae. *PloS one*, *10*(6), pp.e0128376.
58. Wickham, H., 2016. ggplot2: Elegant Graphics for Data Analysis. Springer-Verlag New York.
59. Wright-LaGreca, M., Mackenzie, C. and Green, T.J., 2022. Ocean acidification alters developmental timing and gene expression of ion transport proteins during larval development in resilient and susceptible lineages of the pacific oyster (*Crassostrea gigas*). *Marine Biotechnology*, *24*(1), pp.116-124.
60. Wright, S.H. and Manahan, D.T., 1989. Integumental nutrient uptake by aquatic organisms. *Annual Review of Physiology*, *51*, pp.585-600
61. Van der Schatte Olivier, A., Jones, L., Vay, L.L., Christie, M., Wilson, J. and Malham, S.K., 2020. A global review of the ecosystem services provided by bivalve aquaculture. *Reviews in Aquaculture*, *12*(1), pp.3-25.

Figures

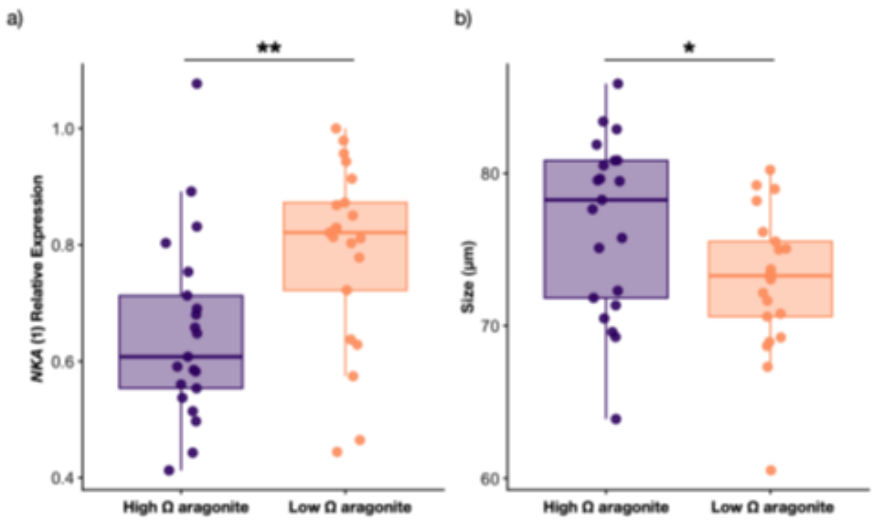


Figure 1

a) *Na^+ K^+ ATPase* [*NKA (1)*] gene expression of oyster larval samples exposed to control or aragonite-undersaturated seawater conditions during the first 24 hrs of life. Expression was measured using a whole-mount fluorescent *in situ* hybridization (wmFISH) method and standardized using the house-keeping gene, *Elongation Factor Unit alpha 1*. b) Size (length in mm) difference between larvae from high and low $W_{Aragonite}$ treatment seawater conditions analyzed for wmFISH analysis. Asterisks indicate significant differences between treatment groups using a Student's *t* test (* indicates $p < 0.05$, ** indicates $p < 0.01$).

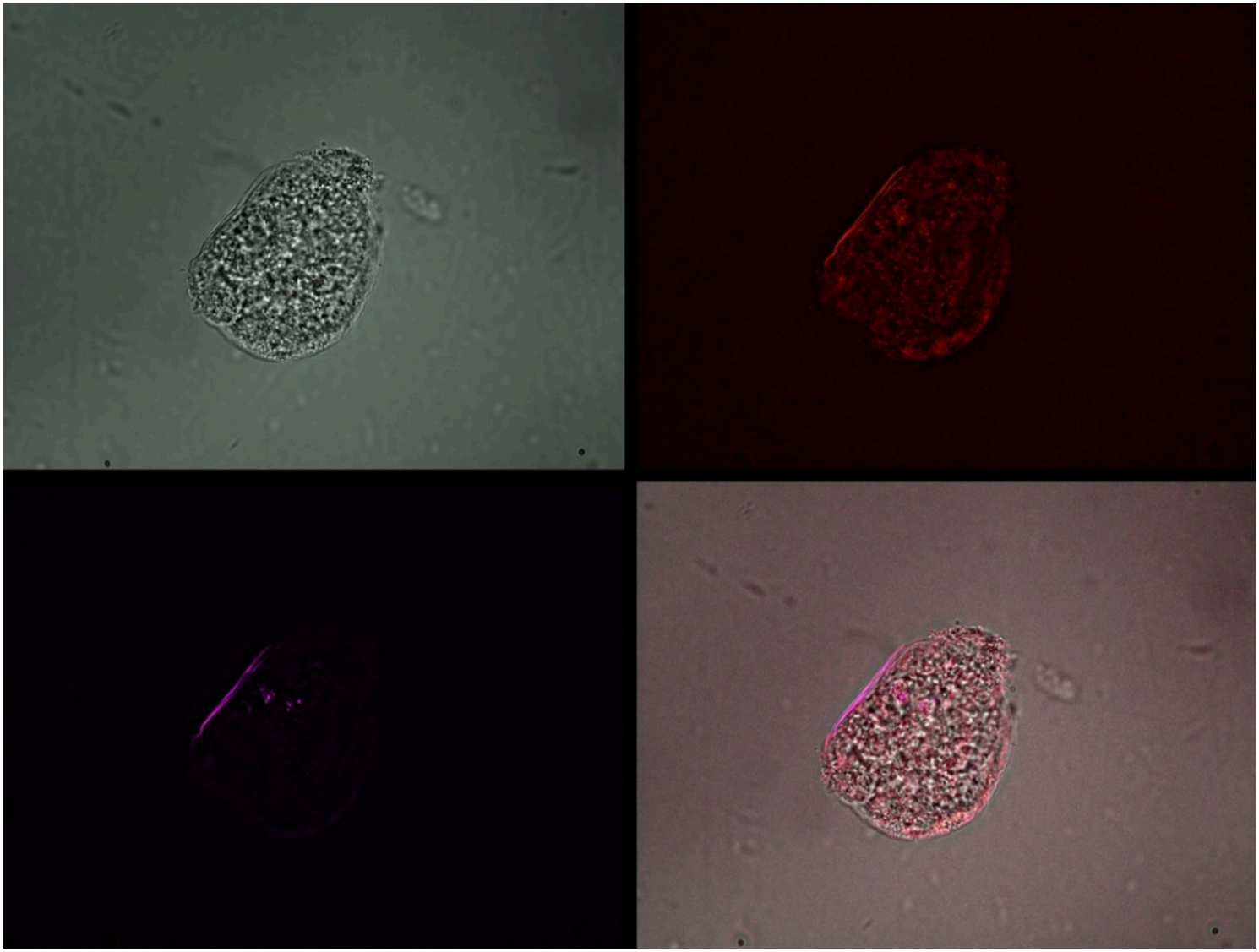


Figure 2

Image of a Pacific oyster larva (24 hrs post-fertilization) characterized with a developed prodissoconch I shell following whole-mount fluorescent *in situ* hybridization with the housekeeping gene, Elongation *factor unit alpha* (red; top right quadrant), and the gene of interest, *Na^+ K^+ ATPase [NKA*] (purple; bottom left quadrant). The top left quadrant is a phase image, and the bottom right is all quadrants combined.

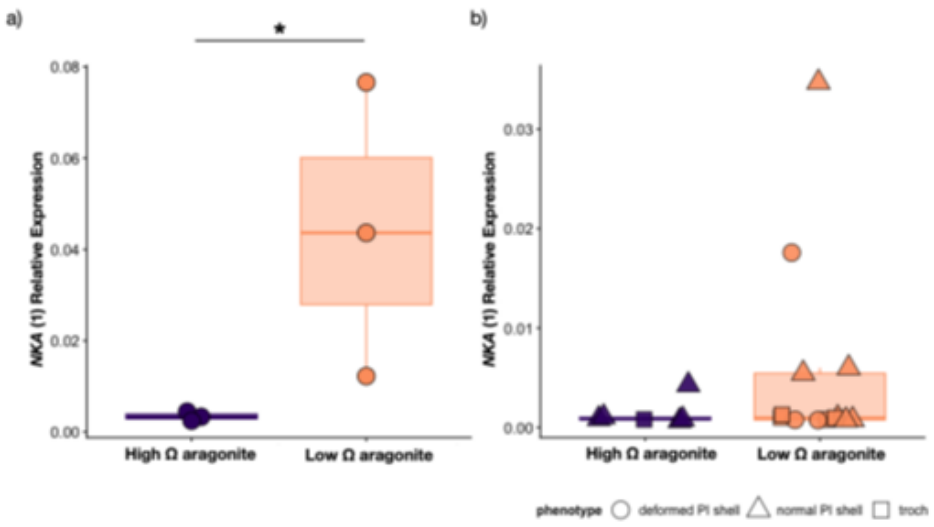


Figure 3

Relative gene expression for a Na^+ K^+ ATPase encoding gene, *NKA (1)*, of *Crassostrea gigas* larvae at 24 hours post-fertilization exposed to high and low $W_{Aragonite}$ conditions using a) pooled larval or b) single larval sampling methods. Single larval sampling methods enabled phenotype-based selection of individual larvae, which were classified as deformed PI shell (high $W_{Aragonite}$: n = 0; low $W_{Aragonite}$: n = 3), normal prodissoconch I (PI) shell (high $W_{Aragonite}$: n = 5; low $W_{Aragonite}$: n = 6), or troch (trochophores) (high $W_{Aragonite}$: n = 1; low $W_{Aragonite}$: n = 3). Asterisks indicate a significant difference (0.05 alpha level) in NKA (1) expression (* $p < 0.05$).

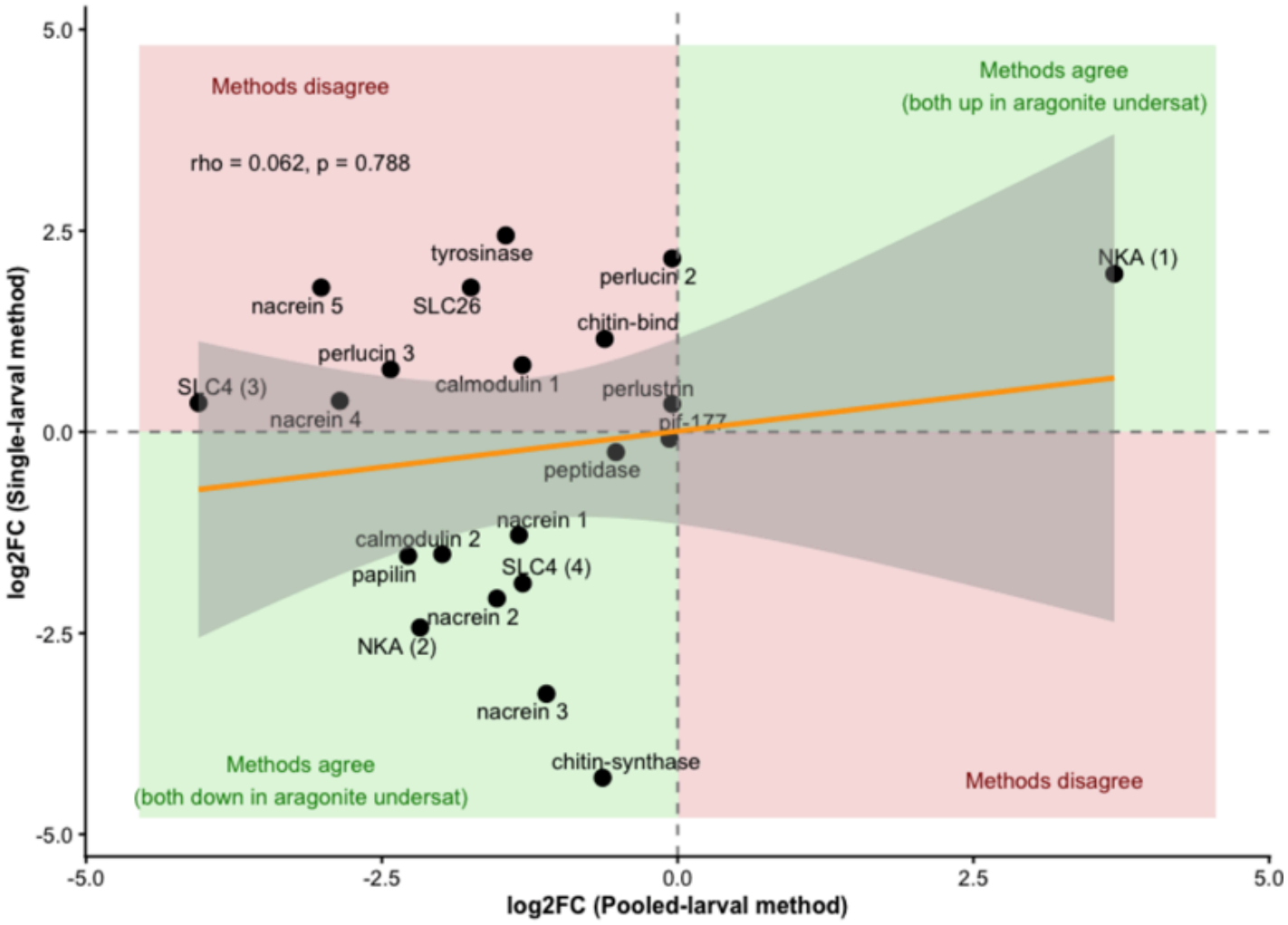


Figure 4

Plot comparing log-fold change in relative expression of selected 21 genes in Pacific oyster larvae (24 hrs post-fertilization) utilizing either a single larval (y axis) or pooled larval sampling method (x axis) for RT-qPCR. Points corresponding to genes in green shaded areas indicate sampling methods agree on gene up or downregulation; whereas points in red shaded areas indicate methods disagree. Aragonite undersat = Aragonite undersaturated ($W_{Aragonite} < 1.7$).

Supplementary Files

This is a list of supplementary files associated with this preprint. Click to download.

- SupplementalVideo1.mp4